Green Synthesized ZnONPs Using Foeniculum vulgare L. Seed Extract and Investigation of Antioxidant Activity in *Ganoderma lucidum*

Z. Khazaei[1], M. Behnamian[1]*, S. Dezhsetan[2], A. Estaji[1]

[1]*Department of Horticultural Sciences, University of Mohaghegh Ardabili, Ardabil, Iran*
[2]*Department of Plant Production and Genetics, University of Mohaghegh Ardabili, Ardabil, Iran*

ABSTRACT

Green nanotechnology is an environmentally friendly method that can reduce the negative impacts of chemical materials on humans and the environment. In this study, aqueous extracts of *Foeniculum vulgare* seed were used for the green synthesis of ZnONPs. The experiment was done in a nutrient solution supplemented with either ZnONPs or bulk ZnO (0, 4, 6 and 8 mM) in two mycelial strains of *Ganoderma lucidum*. To confirm that nanoparticles were synthesized, relevant devices were used, i.e. ultraviolet (UV-Vis) spectroscopy, dynamic light scattering (DLS), Fier conversion infrared spectroscopy (FT-IR), X-ray diffraction (XRD), electron analysis Microscope (SEM) and transmission electron microscope (TEM). The size of ZnONPs varied between 13 and 25 nm. ZnONPs and bulk ZnO were used for evaluating several growth factors, such as diameter and area of the colony, percentage of inhibition, physiological and biochemical traits. The results showed that ZnONPs and bulk ZnO reduced the mycelial growth rate, but significantly increased the contents of MDA (lipid peroxidation), H_2O_2 (hydrogen peroxide), EC (electrolyte leakage), CAT (catalase), SOD (superoxide dismutase) and POD (peroxidase). The concentration of ZnONPs and bulk ZnO, up to 6 mM, increased the activity of antioxidant enzymes, but higher concentrations reduced the activity. ZnONPs and bulk ZnO lowered the rate of mycelial growth in *Ganoderma* by creating oxidative stress. Ultimately, the mycelia acted against the oxidative stress by increasing the production of antioxidants. The results of this study suggest that ZnONPs and bulk ZnO, especially ZnONPs, leads to the improved antioxidant capacity of *Ganoderma*.

KEYWORDS

enzyme activity, *Ganoderma*, mycelial growth, nanoparticles, zinc oxide

Received 29 April 2023, revised 9 February 2024, accepted 8 March 2024

INTRODUCTION

Recently, the synthesis of metal oxide nanoparticles (NPs) has received considerable attention. These NPs bear unique characteristics compared to bulk materials with similar chemical compositions.[1] Nanotechnology is a modern technology that can revolutionize various scientific fields, including agriculture.[2] Nanoparticles are one of the most essential technological tools with specific, physical and chemical attributes that make them stand out compared to their bulk form.[3] Nanoparticles (NPs) possess unique physicochemical features such as particle morphology, tunable pore size, high reactivity, and high surface area[4], nevertheless, the toxicity of NPs is one of the most important factors causing damage to plant's genes, DNA, molecules and other crucial plant functions.[5] Metal oxide nanoparticles are important because of their exceptional surface functionalities. They have different electrically charged structures, as well as biological activities, due to their unique characteristics such as semi-conductance and insulation.[6] Among metal oxides, 528 tons of ZnONP are produced annually in the world. They are one of the most important materials with biocompatible and environmentally friendly properties. In particular, they have been considered useful because of their antimicrobial and antioxidant activities.[7] Zinc is involved in the structure of various enzymes, nucleic acid and protein synthesis, which is necessary for the proper growth of living organisms. A lack of this element can delay growth and ultimately cause reductions in fungal yield. Zinc is needed for fungal enzyme activities, intermediary metabolism, fungal growth and biological cycles.[8] Moreover, zinc acts as an antagonist against heavy metals such as cadmium, nickel and lead, reducing the toxic risk of their high concentrations in some mushrooms.[9] This element is the only transition metal is required for the activity of lyases, isomerases, hydrolases, transferases, oxidoreductases and ligases, in addition to being a precursor for the function of metalloenzymes that are involved in protein and nucleic acid metabolism.[10] The dissolution of Zn nanoparticles in water can result in the production of Zn^{2+} in the medium.[11] It is thought that the positively charged metal binds to negatively charged groups on the surface of cell membranes.[12] In a previous study, a high concentration of Zn was found in a mycorrhizal fungus grown on a polluted substrate, so most of the Zn was located extrahyphally and bound to the cell wall or extracellular slime polymers.[13] It was reported that extracellular slime components contain electronegative sites through which zinc ions can bind to cell walls.[14] Considering the vital role of the cell wall in the binding of metals, metal ions can bind to the cell wall in different ways, depending on the composition of the cell wall.[15] It has been suggested that Zn can have a negative effect on growth by interfering with the function of cell walls. This may occur due to blockade in cellular reactions and metabolic pathways, since an increase in Zn concentration in the culture medium could cause a decrease in fungal biomass.[16] Therefore, elevated concentrations of Zn may have an inhibitory or toxic effect on cellular activity and growth,[11] thereby impeding the production of extracellular enzymes.[17] This chain of events can adversely affect the cycling of carbon and nutrients.[18]

It is reported that the use of metal nanoparticles may disrupt intracellular metabolism[19] or may damage the antioxidant defense system,[20] thereby causing an accumulation of reactive oxidative species (ROS). While ROS usually play essential roles in signaling and homeostasis,[21] an excessive accumulation of ROS often leads to oxidative stress. It can damage lipids, proteins, carbohydrates and DNA, which could eventually result in cell death.[22] Moreover, high ROS content can instigate lipid peroxidation, as this is detectable by the accumulation of malondialdehyde in cells.[23] Naturally, the toxic effects of oxidative stress can be overcome by enzymatic antioxidants

*To whom correspondence should be addressed
Email: mbehnamian@uma.ac.ir

ISSN 1996-840X Online / South African Chemical Institute / https://saci.co.za/journal

https://doi.org/10.17159/0379-4350/2024/v78a20

such as (POD), (CAT) and SOD and non-enzymatic ones such as proline which play vital roles in the defense system.[24] SOD has been considered the first enzyme in the line of cellular defense, tasked with attacking oxygen radicals (O^-) and catalyzing them to hydrogen peroxide to protect cells against oxygen-derived free radicals.[25] Then, CAT converts hydrogen peroxide (H_2O_2) into H_2O and O_2.[26] POD is usually seen as another enzyme in the detoxifying of H_2O_2 since it functions through various electron donors,[27]while proline serves as a non-enzymatic antioxidant in ROS scavenging.[28]

Ganoderma lucidum is a mushroom with a glossy exterior and a woody texture.[29] Its nutritional components include protein, fats, carbohydrates, fiber and vitamins, as well as several minerals such as calcium, potassium, magnesium, phosphorus, iron, selenium, copper, and zinc.[29] In China and several European countries, this mushroom is considered a supplement for cancer treatment due to its potent antioxidant activity and ability to counter the side effects of chemotherapy.[30] This high antioxidant capacity in *Ganoderma* and its ability to stop lipid peroxidation create a balance between ROS production and the antioxidant defense system, which leads to a reduction in oxidative stress.[31] The proteins in *Ganoderma* contain all of the essential amino acids, especially the lysine and leucine, associated with a high amount of polyunsaturated fatty acids and a low amount of total fat.[32]

While the use of nanoparticles in the food industry is becoming more and more popular among scientists, the current modes of nanoparticle synthesis are physical, chemical, or green. The physical and chemical modes of synthesis are expensive and require access to expensive, sometimes complicated equipment, while needing the provision of special conditions such as high temperature and pressure. Chemical compounds that can be toxic to the health of living organisms[33] have prompted researchers to formulate safe, low-cost methods for the synthesis of nanoparticles.[34] The term "green" in this article and in the available literature is synonymous with the application of methods and materials that render the synthesis of a compound environmentally-friendly. So far, different parts of plants[35] and fungi[36] have been tested for the synthesis of ZnONPs.[37]

Plant extracts in the process of nanoparticle synthesis, act as reducing, stabilizing agents for the synthesized nanoparticles, whereas in chemical synthesis the use of toxic chemicals can lead to hazardous wastes.[38] Using plant extracts in these procedures has brought advantages in terms of interactions with and effects on environments.[39]Thus, plant extracts are an optimal option for the synthesising of NPs, since they do not contain toxic chemicals.[37] Accordingly, in the present research, the green synthesis of metal nanoparticles occurred through synthesizing ZnONPs, along with using the seed extract of *Foeniculum vulgare*, a medicinal plant. Ultimately, the effects of ZnONPs were evaluated on the antioxidant capacity of *Ganoderma lucidum*. The hypothesis was that ZnONPs could increase the production of antioxidants in the mycelia of *G. lucidum*.

MATERIALS AND METHODS

Chemicals and Reagents

The chemicals that were used in the experiments of this research were, namely, Zn $(NO_3)_2.6H_2O$, ZnO, NaOH and malt extract agar (MEA). All were purchased from Merck, Germany.

Preparation of *Foeniculum vulgare* seed extract

Dried seeds of *Foeniculum vulgare* Mill. Finocchio Montebianco Italian cultivar was purchased from an online market and was used for the green synthesis of zinc nanoparticles. The seeds were first rinsed in water, and then 100 g of dried seeds were powdered and mixed with 200 ml of deionized water. The solution was heated to 60 °C and kept there for 1 hour before filtering by centrifugation at 4500 g. The extract was stored in the refrigerator at 4 °C until further use.[38]

Preparation of *Ganoderma lucidum*

Ganoderma lucidum strains (G01 and G16) were obtained from a mushroom laboratory at the University of Mohaghegh Ardabili. The fungi were certified by an expert in verifying the genus and species.

Green synthesis of ZnONPs

To synthesize the ZnONPs, 50 ml of aqueous extract was obtained from *Foeniculum vulgare* seeds and mixed with 50 ml of deionized water. Then, zinc nitrate (6.4 g) was added to the diluted extract solution and stirred at room temperature for 20 min. After complete dissolution, the pH was adjusted to 12, using 5 M NaOH, and the solution was stirred for 1 hour until yellow sediments appeared. The sediments were washed several times with deionized water to be purified and then centrifuged at 3000 g (10 min, 25 °C). To remove the impurities from the sediments, the samples were heated in an electric furnace at 500 °C for 2 hours. After drying, the color of the sediments changed from yellow to white which indicated that ZnONPs had formed.[40]

Characterization of ZnONPs

The size and morphology of ZnONPs were evaluated by SEM (LEO 1430VP(and TEM (Philips-EM208S, acceleration voltage: 100 kV). The XRD pattern was recorded by a GNR Italstructures MPD 3000 using CuKα radiation (λ= 0.15406 nm; scanning rate: 0.04˚/sec in the 2θ range from 20˚ to 80˚). The Scinco 4100 was used for recording the DRS spectrum. The particle sizes of ZnONPs were detected by DLS (HORIBA Scientific, nanopartica, SZ-100). Monitoring the chemical structure of the synthesized nanoparticles was done by FTIR (Perkin Elmer Spectrum RX I, USA) and the infrared spectra operated at 400-4000 cm^{-1}.

Preparation of culture media and assessment of mycelial growth

Malt extract agar was used as the base culture medium. After autoclaving at 121°C for 15 minutes, the culture medium was allowed to cool slightly under the laminar airflow. Then, ZnONPs were added to the media at different concentrations (i.e. 0, 4, 6 and 8 mM), and the media were inoculated with *Ganoderma lucidum*. The culture media without nanoparticles were considered as the control treatment.

The vegetative growth of *Ganoderma lucidum* was evaluated by measuring the mycelial diameter (mm) along two perpendicular directions and by monitoring the colony area (mm^2) simultaneously and daily, until the Petri dishes became utterly full of the fungi in control samples. The following formula was for calculating the inhibition ratio. A concentration that caused more than 20% inhibition was considered as an inhibitory concentration:[41]

$$\text{Inhibition ratio (\%)} = (C - E)/C \times 100\% \quad (1)$$

Where C was the average diameter of the largest and smallest mycelia of the untreated (control) samples, and E was the average diameter of the largest and smallest mycelia of the treated samples.

Linear regression was used for calculating the IC_{50}.[42]

The liquid culture medium comprised glucose (35 g L^{-1}), peptone (5 g L^{-1}), yeast extract (2.5 g L^{-1}), KH_2PO_4 (0.883 g L^{-1}), Vitamin B_1 (0.05 g L^{-1}) and $MgSO_4.7H_2O$ (0.5 g L^{-1}). The pH value remained at 5.5 and the culture medium was used for producing a suitable quantity of mycelium that could enable the measurement of enzymatic properties. Then, ZnONPs were added to the media (100 mL) at different concentrations (i.e. 0, 4, 6 and 8 mM) and inoculated with *Ganoderma lucidum*. The cultures were placed on a rotary shaker (80 g, 28 °C, for periods of 4, 6 and 8 days) and, at the end of each period, the collected mycelia were used for evaluating enzymatic activity.[42]

Proline content

The proline content was determined according to Bates et al. (1973)[13]. In brief, 0.2 g of mycelium was ground with a mortar and pestle in sulfosalicylic acid (3%), and was then centrifuged (14000 g, 15 min, 25 °C). Two mL of the supernatant was mixed with glacial acetic acid (2 mL) and ninhydrin solution (2 mL; 1.25 g ninhydrin in 20 ml 6-orthophosphoric acid). The solution was heated for one hour to reach 100 °C, and was then cooled at room temperature. Subsequently, toluene (5 mL) was added and the solution was vortexed for 20 s. After 10 min, the phases were separated and the absorbance values were read at 520 nm. Proline content was presented as μg g^{-1} FW.

Malondialdehyde (MDA) content

The MDA content was determined according to Wang et al. (2019)[43] with some modifications. In brief, 0.5 g of the mushroom cap was homogenized with trichloroacetic acid (5% w/v, 5 mL) in an ice bath and was then centrifuged (10000 g, 15 min at 4 °C). The supernatant (2 mL) was mixed with trichloroacetic acid (5% w/v, containing 0.67% thiobarbituric acid, 2 mL) and was stored in a Bain-marie (5 min, 95 °C). The solutions were then cooled rapidly and the absorption values were recorded at 450, 523 and 600 nm. MDA was presented as μmol g^{-1} FW.

Electrical conductivity (EC)

The electrical conductivity was determined according to Liu et al. (2020).[44] Two grams of mycelium were washed with distilled water (three times) and dried on filter paper. Then, the collected mycelia were suspended in distilled water (25 mL) and kept on a rotary shaker (25°C, 30 min) before measuring electrical conductivity (EC1). After heating the samples in Bain-marie (boiling water, 15 min), they were allowed to cool at room temperature, and then the electrical conductivity was measured again (EC_2). The EC value was calculated by the following formula:

$$EC\ (\%) = EC_1/EC_2 \times 100 \quad (2)$$

H_2O_2 content

The H_2O_2 content was determined by a suitable method by Liu et al. (2020)[44] with some modifications. One gram of mycelium was homogenized in TCA (1% w/v, 5 mL) in an ice bath, and was then centrifuged (10000 g, 20 min, 4 °C). One mL of supernatant was mixed with potassium phosphate (1 mL, 0.1 M, pH 7) and potassium iodide (1 mL, 1 M). The reaction mixture was kept in the dark (1 hour, 25 °C) and the absorbance was measured at 390 nm. A standard curve was constructed using different concentrations of H_2O_2 and presented as μmol g^{-1} FW.

Assaying antioxidant enzyme activity

Extraction of crude enzyme

To evaluate the enzymatic activity, 0.3 g of mycelium was homogenized in potassium phosphate (PPB) buffer (5 mL, 50 mM, pH 7) containing EDTA (1 mM) and PVP (1%) before being centrifuged (15000 g, 20 min, 4 °C). The supernatant was immediately used for CAT, SOD and POD assays.[45]

Enzymatic activity assay

To determine CAT activity, crude enzyme (0.15 mL) was mixed with PPB (1 mL, 100 mM, pH 7.8) and H_2O_2 (1.5 mL, 15 mM). Changes in the absorbance values of the solutions were recorded at 240 nm, and the enzyme activity was expressed as Ug^{-1} FW. [47]

The SOD activity was measured according to a method according to Xia et al. (2008).[46] In brief, 0.2 mL of the crude enzyme was added to potassium phosphate buffer (1 mL, 100 mM, pH 7.8), methionine (0.7 mL, 55 mM), nitroblue tetrazolium (0.3 mL, 0.75 mM) and riboflavin (0.6 mL, 0.1 mM). The solutions were irradiated by fluorescent light (40 μmol m^{-2} s^{-1}, 10 min). The absorbance of the samples was recorded at 560 nm and expressed as Ug^{-1} FW.

The POD activity was assayed according to a method by Zhou and Leul (1998).[47] The reaction mixture consisted of crude enzyme (0.5 mL), guaiacol (5mM) in sodium phosphate buffer (1 mL, 50 mM, pH 6), and H_2O_2 (1 mL, 5 mM). The absorbance was read at 470 nm and POD activity was presented as Ug^{-1} FW.

Statistical analysis

The practical part of this research was performed as a factorial experiment in a completely randomized design. In this experiment, data were analyzed by SPSS software 18.1 and SNK test. The analyses were carried out by one-way analysis of variance (ANOVA).

RESULTS

UV–Visible spectroscopy analysis

The UV-Vis DRS absorption spectrum provided valuable information. Nanoparticles showed electron adsorption with unique properties. Figure 1a represents the UV-Vis absorption spectrum of the ZnONPs at a wavelength range of 250-800 nm, while an absorption peak was recorded at 370 nm. In Figure1b, the band gap energy of zinc oxide is 3.3eV.

XRD analysis

The XRD pattern of green ZnO-synthesized nanoparticles (Figure 2) showed that all peaks in the diffraction patterns confirmed clearly the hexagonal phase (wurtzite structure) of ZnO and were fully consistent with standard data (JCPDS 36-1451).

SEM and TEM analysis

SEM (Figure 3a) and TEM (Figure 3b) imaging technologies were used for evaluating the shape, structure and size of green-synthesized

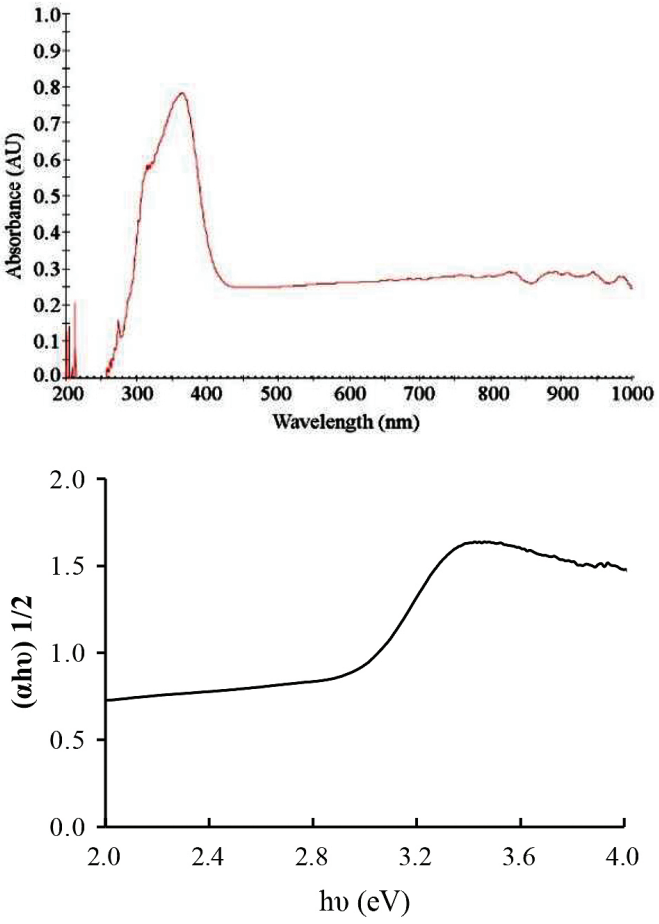

Figure 1. UV–Vis DR spectrum (a) and band–gap (b) of ZnONPs synthesized using ***F. vulgare*** seed extract.

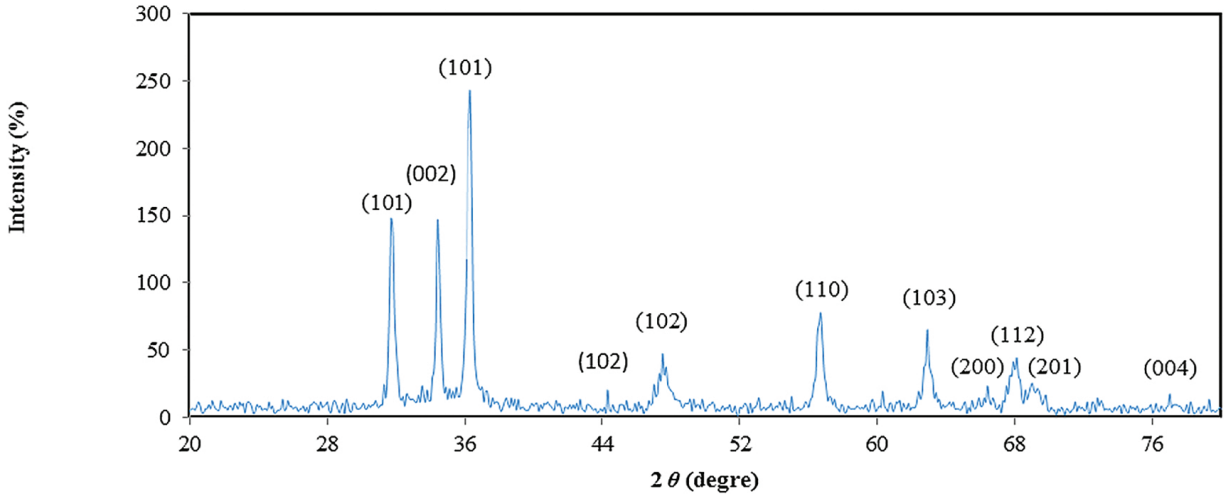

Figure 2. X-RD pattern of ZnONPs synthesized using *F. vulgare* seed extract.

ZnONPs. The results indicated that the shape of ZnONPs was spherical and had a uniform distribution, with an average particle size of 13 to 25 nm.

DLS analysis

DLS analysis confirmed the presence of nanoparticles in the solution and assisted with the evaluation of their particle dispersion. The average size of the synthesized nanoparticles was 126.04 (Figure 4). In this study, the zeta potential of the green-synthesized ZnONPs was -20.5 mV, which indicated the occurrence of stability between the particles (Figure 4).

FT-IR Analysis

The FTIR spectrum of green-synthesized ZnONPs and that of *Foeniculum vulgare* seed extract (Figure 5) revealed the presence of functional groups in the green ZnONPs. The absorption peaks formed at 400–600 cm^{-1} and, thus, confirmed that the Zn–O bond was present in the green-synthesized ZnONPs.

Effect of ZnO NPs and bulk ZnO on Growth of *Ganoderma* mycelium

ZnONPs and bulk ZnO had significant effects on growth parameters of the *Ganoderma* strains, including diameter (Figure 6a) and area of colony (Figure 6b). The results revealed that higher concentrations of ZnONPs and bulk ZnO were more effective in reducing the growth of mycelium, compared to the control (untreated samples).

Proline content

The amount of proline in both strains increased parallel to higher concentrations of bulk ZnO and ZnONPs, but ZnONPs induced

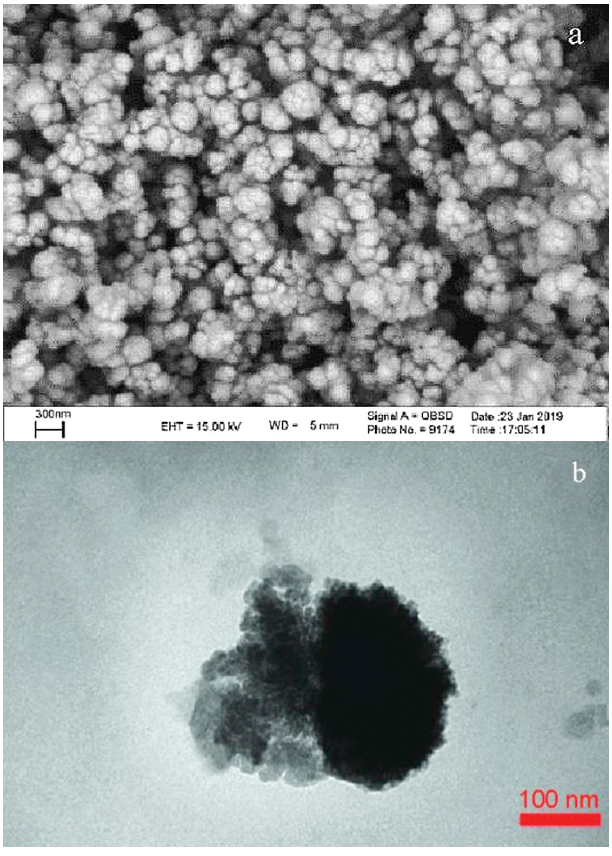

Figure 3. SEM (a) and TEM (b) images of the ZnONPs synthesized using *F. vulgare* seed extract.

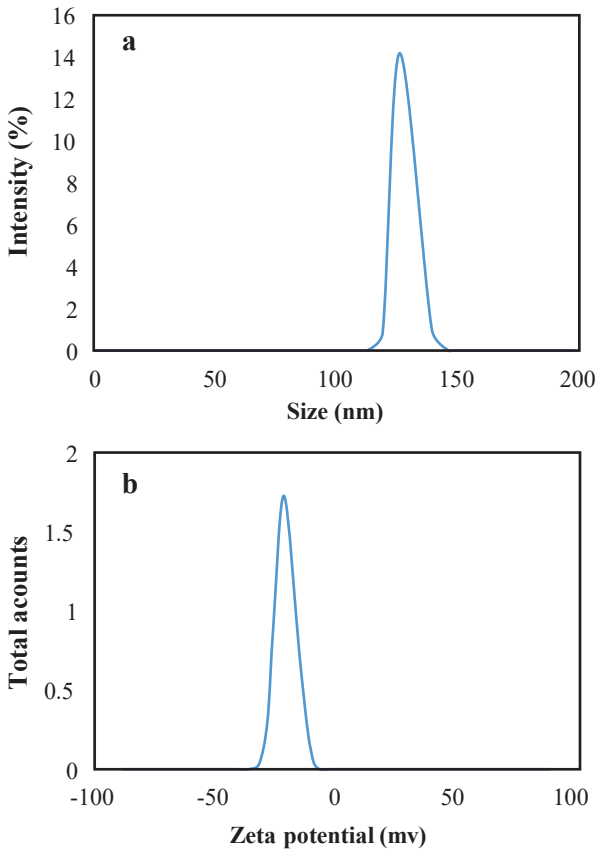

Figure 4. Particle diameter (a) and Zeta potential (b) of ZnONPs obtained by DLS analysis based on intensity.

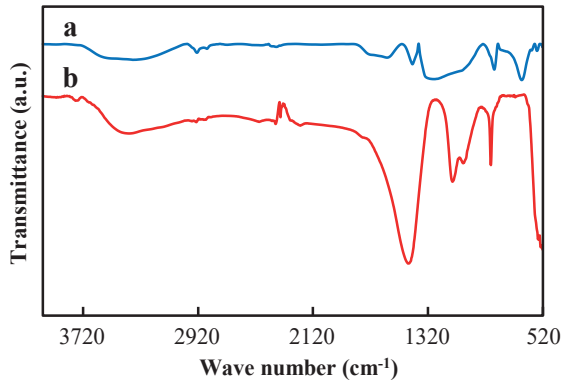

Figure 5. FT-IR spectra of ZnONPs (a) and *Foeniculum* vulgare seed extract (b).

a higher content of proline, compared to the effect of equal concentrations of bulk ZnO, while no significant difference was observed between the strains ($p \leq 0.01$). The maximum increase in proline amount was observed in the G16 strain, which was treated with the highest concentration of ZnONPs, while the least proline content was recorded in the untreated G01 strain (Figure 7a).

MDA content

To evaluate the oxidative stress content in response to ZnONPs and bulk ZnO treatments, the MDA content was measured. The MDA content of the mycelium increased significantly in the strains of *G. lucidum*, parallel to increasing concentrations of bulk ZnO and ZnONPs, as compared to the control treatment ($p \leq 0.01$) (Figure 7b).

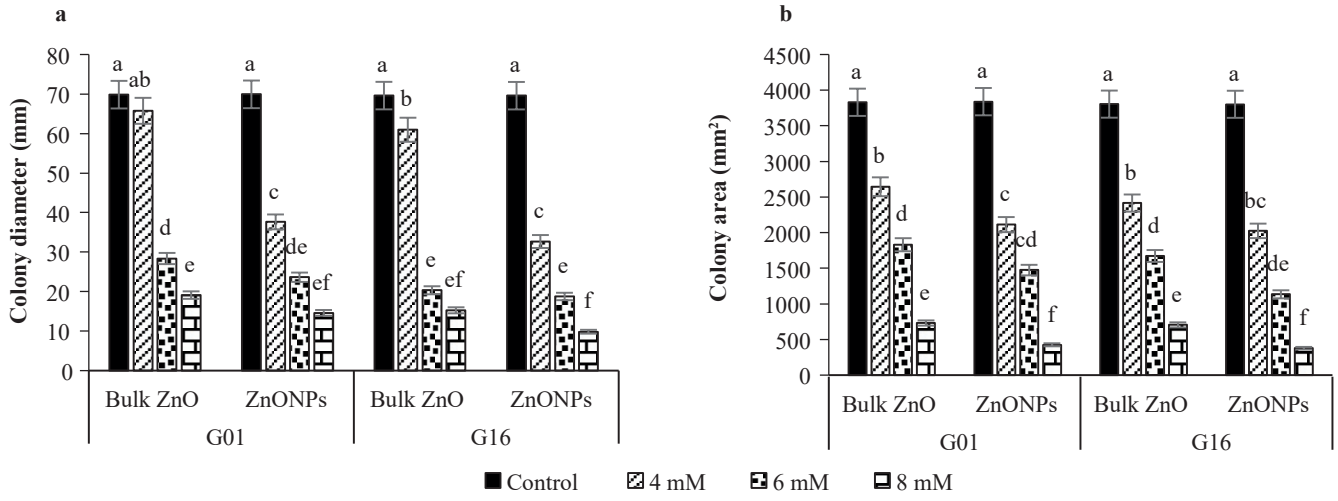

Figure 6. The effect of bulk ZnO and ZnONPs on colony diameter (a) and colony area (b) of two wild strains of *Ganoderma lucidum*.

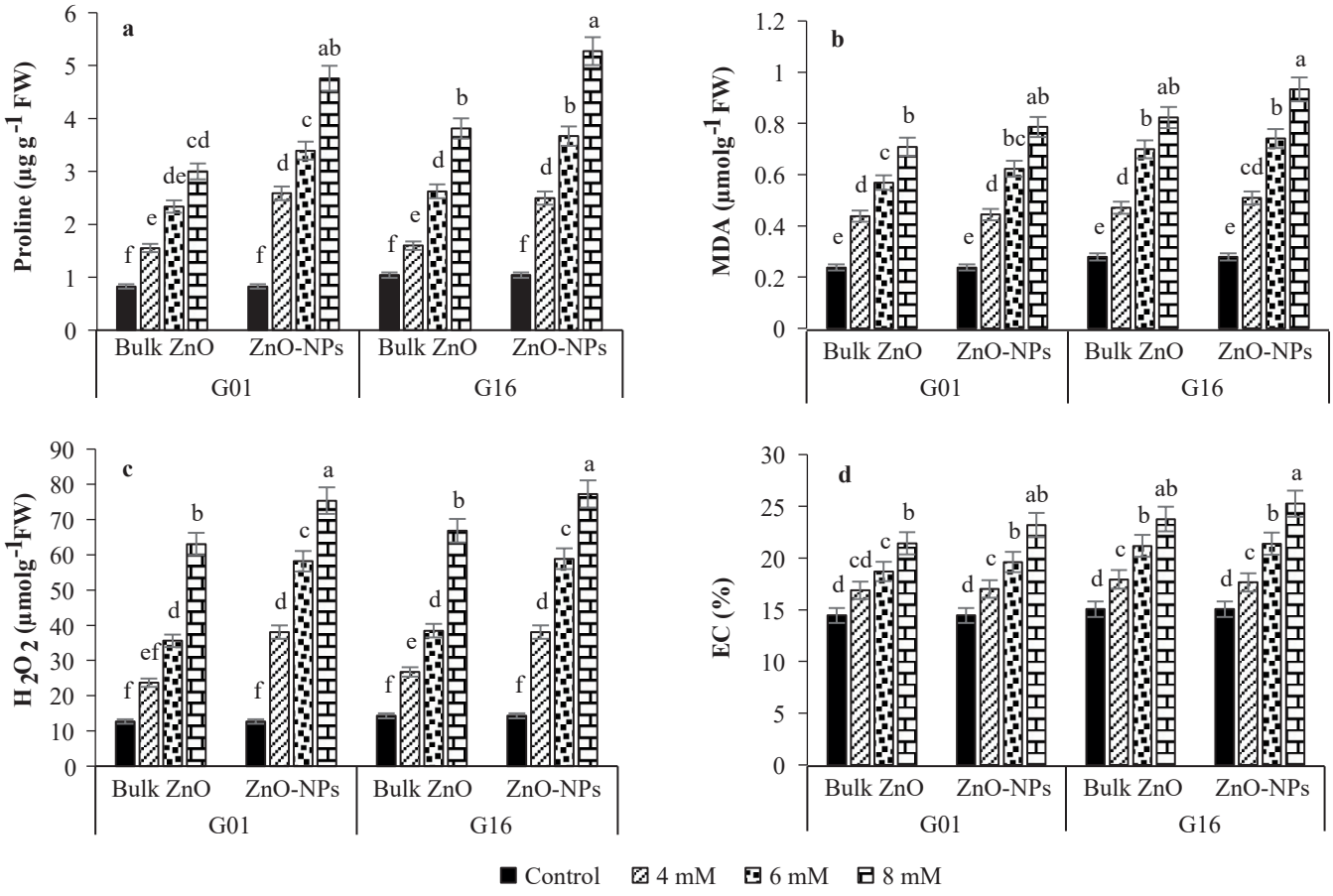

Figure 7. The effect of bulk ZnO and ZnONPs on proline (a), MDA (b), H_2O_2 (c) and EC (d) of two wild strains of *Ganoderma lucidum*.

H_2O_2 content

Bulk ZnO and ZnONPs significantly affected the content of H_2O_2 in the strains of *G. lucidum* ($p \leq 0.01$), since the increase in concentrations of bulk ZnO and ZnONPs resulted in significant enhancements of H_2O_2 content, compared to the control treatment. Nonetheless, there was no significant difference between the studied strains. The highest amount of H_2O_2 was observed in response to the 8 mM ZnONPs concentration in the G16 strain, whereas the lowest amount was found in the control (untreated samples) (Figure 7c).

Electrical conductivity (EC)

The results showed that the EC of media, containing *Ganoderma lucidum*, increased significantly in response to different concentrations of bulk ZnO and ZnONPs, compared to the control ($p \leq 0.01$). ZnONPs affected the EC of cultures more than ZnO, since the highest value of EC was observed in response to 8 mM ZnONPs in the G16 strain, whereas the lowest was obtained from untreated samples (Figure 7d).

Activity of antioxidant enzymes

The results clearly revealed a significant difference between treatments with regard to their effects on the activity of antioxidative enzymes, including CAT, SOD and POD ($p \leq 0.01$). Parallel to increasing the concentrations of bulk ZnO and ZnONPs to 6 mM, there were increases in enzyme activities. However, they decreased in response to the concentration of 8 mM (Figure 8 a, b, c and Figure 9).

DISCUSSION

UV–Visible spectroscopy analysis

In UV-Vis absorption spectrum of the ZnONPs, an absorption peak was recorded at 370 nm, thereby confirming that ZnONPs had formed (Figure 1a).

In previous cases of research, the green synthesis of ZnONPs made absorption peaks for ZnONPs at 382 nm[48] and 370.[49] Our findings showed that the constituents of *Foeniculum vulgare* seed extract had polyphenolic compounds which played a key role as a bioreductant in the green synthesis of ZnONPs. In the main band gap of the nanoparticle band, there was a transfer of electrons from the voltage to the transmission band, $Zn_3d \rightarrow O_2p$ which resulted in a peak. The optical band-gap of the synthesized nanoparticle band was calculated by the following formula Tauc ($\alpha h\upsilon$) 2 = A ($h\upsilon$ – Eg), where α is the adsorption coefficient, h is the constant platelet, υ is the photon frequency, A is proportional to the constant and Eg is the optical band gap of energy.[50] In Figure1b, the band gap energy of zinc oxide is 3.3eV.

XRD analysis

The XRD pattern of green ZnO-synthesized nanoparticles showed that all peaks in the diffraction patterns confirmed clearly the hexagonal phase (wurtzite structure) of ZnO (Figure 2). The diffraction peaks of the synthesized ZnONPs at 2θ = 31.7°, 34.4°, 36.3°, 47.5°, 56.7°, 62.9°, 66.4°, 68.1°, 69.2° and 77.2° were indexed to (100), (002), (101), (102), (110), (103), (200), (112), (201) and (004), respectively.[50] This result confirmed that green-synthesized ZnO nanoparticles were crystalline in nature and had negligible impurities. Using the XRD pattern, the diameters of ZnONPs were determined from the Debye -Scherer equation:

$$D = k\lambda/\beta\cos\theta \quad (3)$$

Where D was the ZnONPs crystallite size (nm), k was a dimensionless shape factor (0.9), λ was CuKα radiation (1.54 Å), θ was the diffraction angle, and β was the full width at half-value of the maximum peak diffraction (FWHM).[48] Using the above formula, the synthesized zinc oxide nanoparticles had an average size of 24 nm.

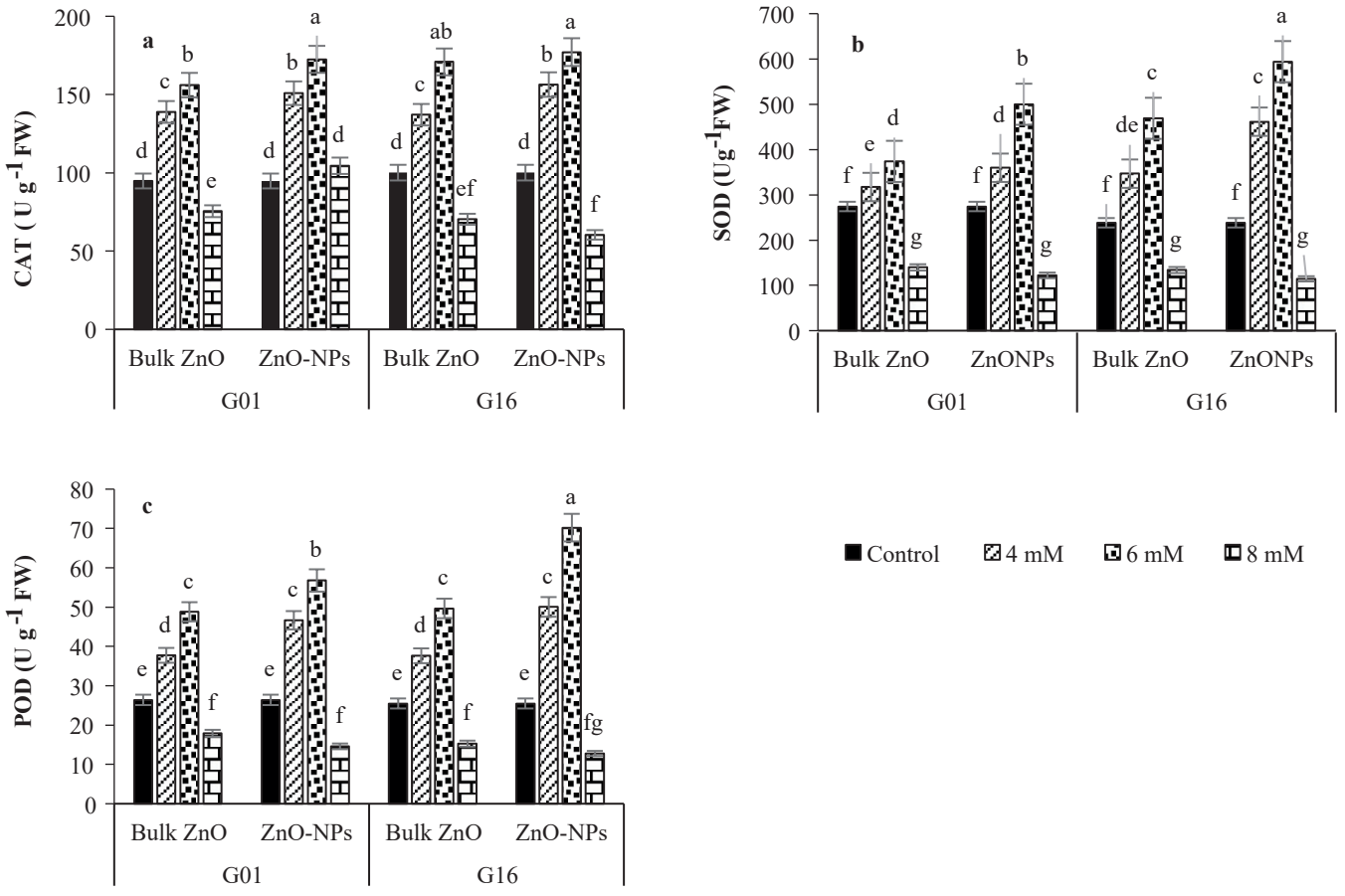

Figure 8. The effect of bulk ZnO and ZnONPs on CAT (a), SOD (b) and POD (c) activity of two wild strains of *Ganoderma lucidum*.

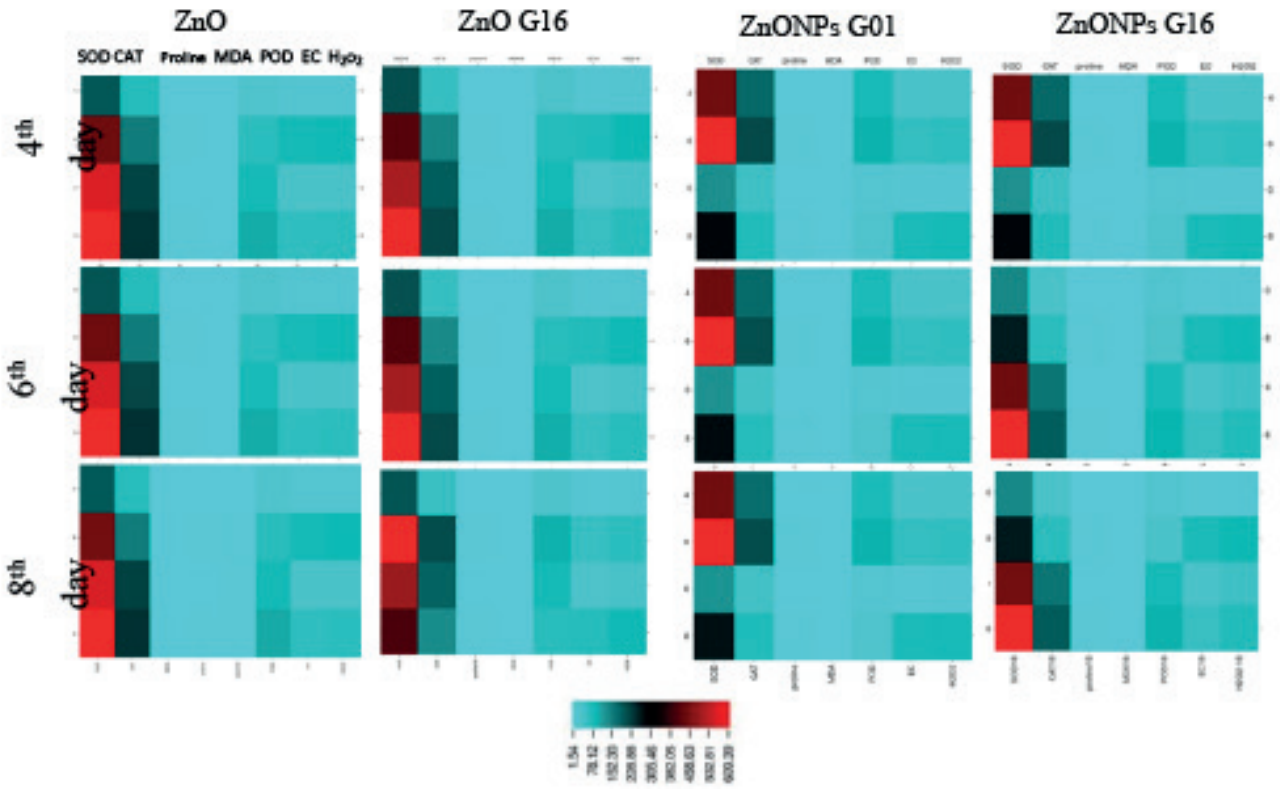

Figure 9. Heatmap showing the effect bulk ZnO and ZnONPs after 4, 6 and 8 days with different treatments (0, 4, 6 and 8 mM) in two wild strains of *Ganoderma lucidum* (G16 and 01)

SEM and TEM analysis

SEM and TEM imaging indicated that the shape of ZnONPs was spherical and had a uniform distribution, with an average particle size of 13 to 25 nm respectively (Figure 2a and 2b). However, nanoparticles with larger sizes were also observed, possibly due to the accumulation of smaller nanoparticles Nascimento et al. (2020) as a result of polarization and electrostatic adsorption of ZnONPs.[51]

TEM images revealed that the green ZnONPs were polycrystalline in nature and spherical in shape. While different plants constitute different types and amounts of chemicals, their ability to react and reduce other compounds can be variable.[48] Different values were obtained from the TEM analysis of the synthesized ZnONPs (compared to XRD), which may indicate that this analysis can discriminate distances between the particles. Meanwhile, the XRD analysis revealed a crystalline region with the ability to diffract X-rays.

DLS analysis

The average size of the synthesized nanoparticles was 126.04 (Figure 2c) which was consistent with previous cases of green-synthesized ZnONPs using *Lactobacillus plantarum* (124.2 nm).[52]

Research on zeta potential previously identified the particle size distribution and the stability of nanoparticles.[52] The synthesized nanoparticles, which are dry powders, can form agglomerates or aggregates in a liquid medium. Agglomerates are a group of primary particles that accumulate together by a weak Vander Waals force. Meanwhile, "aggregate" refers to a mass of primary particles that are held together by strong chemical bonds.[53] In this study, the zeta potential of the green-synthesized ZnONPs was -20.5 mV, which indicated the occurrence of stability between the particles (Figure 2d). A relevant study showed that the zeta potential for ZnONPs was -21.5 mV.[54] In another study Rao and Shekhawat (2014),[55] suggested that negative and large amounts of Zeta potential in an aqueous medium usually resulted from repulsions between particles, which increased the stability between ZnONPs. Also, this amount of negative charge in and among the green synthesized nanoparticles reflected the presence of flavonoids and other phenolic compounds which had a reductive role in the extract. In general, it can be stated that this large negative charge indicates the presence of a strong static electric force between the synthesized particles.[54]

FT-IR Analysis

The absorption peaks formed at 400–600 cm^{-1} (Figure 3a, b) and, thus, confirmed that the Zn–O bond was present in the green-synthesized ZnONPs.[34] The absorption of the FTIR spectrum in the case of zinc oxide nanoparticles was 466 cm^{-1}, which confirmed findings from a previous study.[56] The broad peak at 3410 cm^{-1} related to H-stretched and O-H traction modes. The O-H tensile band indicated the presence of compounds such as hydroxyl, alcohol and phenol.[57] Peaks of 1150 cm^{-1} and 1074 cm^{-1} belonged to the C-O bond which is involved in the formation of alcohols, ethers, carboxylic acids and esters. The 1450 cm^{-1} peak could be attributed to the C-H bond, as generated by strong adsorption.[57] Absorbent peaks in the range of 2346.43 cm^{-1} and 2380 cm^{-1} reflected the presence of CO_2 molecules in the air and, thus, can be ignored because of their negligible role.[58] Finally, the absorption peak observed at 882 cm^{-1} related to the C-H band of aromatic compounds.[59] In a previous research Mateo et al. (2015)[60] showed that the FT-IR technique of ZnONPs, during the synthesis process, stabilized the surface of nanoparticles and maintained the accumulation of *P. granatum* compounds.

FTIR spectra of *Foeniculum vulgare* seed extracts exhibited a set of broad IR absorption bands at 3371.79 cm^{-1}, 2927.66 cm^{-1}, 1604.57 cm^{-1}, 1427.80 cm^{-1}, 1274.07 cm^{-1}, 858.41 cm^{-1}, 667.45 cm^{-1}, 561.19 cm^{-1} and 508.82 cm^{-1}. The broad peak was identified at 3371.79 cm^{-1} which could be attributed to hydrogen-bonded phenolic groups of phyto-constituents.[55,61,62] A peak at 2927.66 cm^{-1} was relevant to the C≡C bond which is involved in the formation of alkynes. The absorption peak at 1604.57 cm^{-1} was assigned to the C=O of amides.[55,61] The absorption peak at 1427.80 cm^{-1} was attributed to the C-H band.[55,61] The absorbance peak at 1274.07 cm^{-1} was relevant to the C-O bond which is involved in the formation of aromatic compounds.[61] A broad peak at 858.41 cm^{-1} was assigned

to the C-H bond.[55] A peak at 667.45 cm^{-1} related to the C-H band of aromatic rings, as also stated in a previous study Ali et al. (2018)[2] and, finally, two peaks at 561.19 and 508.82 were attributed to the C-Br band of alkyl halide.[55]

Effect of ZnO NPs and bulk ZnO on Growth of *Ganoderma* mycelium

ZnO had a significant inhibitory effect on the growth of *Ganoderma lucidum* (Figure 4a, b). This inhibitory effect could be attributed to the toxicity of ZnO and to the production of reactive oxygen species on the surface of these particles. Since electron-related properties of nanoparticles are unique, they can disrupt the electron transfer processes in biological systems within the inner membrane of mitochondria.[63] The ZnO surface is able to react with H_2O and can result in the creation of OH radicals, as well as H_2O_2.[64] Previous studies have shown the impact of ZnONPs on *Erythricium salmonicolor* and bulk ZnO on *M. citricolor*.[65-66] In particular, these particles adversely affected growth parameters, thereby confirming our findings in the current research. The IC50 value for the G01 strain regarding ZnONP was 4.26 mM and, for bulk ZnO, the value was 4.71 mM. Meanwhile, the IC50 value for the G16 strain regarding ZnONP was 4.28 mM and, for bulk ZnO, the value was 4.72 mM (Figure 10). These indications make it reasonable to state that increasing the concentration of ZnONP and bulk ZnO types can inhibit the growth rate by up to 50%.

Proline content

Enhanced content of proline in response to stress usually denote a defense mechanism that can result from enhanced content of proline synthesis or a decrease in its degradation.[67] Under stress conditions, such as exposure to heavy metals, proline acts as a metal chelator, osmoprotectant and ROS quencher. In this way, it protects the cells from damage caused by stress.[68] It also stabilizes intracellular structures such as proteins and cell membranes, scavenges free radicals, and plays a role in buffering redox potential.[69] In previous cases of research, ZnONPs increased proline content in *Brassica juncea* when used at a concentration of 1000 mg/L.[70] Bulk types and nanoparticles of ZnO and CuO)1µM) affected the proline content in *Glycyrrhiza glabra*.[70] In another study, Faizan et al. (2018)[29] reported that ZnONPs and bulk ZnO had significant effects on proline content, in a manner that increasing the ZnONPs and bulk ZnO concentrations caused a corresponding increase in the amount of proline. This increase in the proline content is a programmed response to modulate and reduce oxidative damage to the cells.[71] Although no reports exist on the use of ZnONPs in fungi, and while there are no reports on how it affects proline, our findings on the said effects can be confirmed in the case of *G. lucidum* (Figure 7).

MDA content

One of the most obvious signs of oxidative stress is the changes that occur in lipid peroxidation. It is suggested that abiotic stress, as a result of exposure to heavy metals, can help convert H_2O_2 and O_2 to OH free radicals. These free radicals are highly reactive and cause lipid peroxidation which can be determined by measuring the content of MDA.[67] ZnONPs in *Phaseolus vulgaris* and flax caused changes in the level of MDA and increased the level of lipid peroxidation which is compatible with our results in *Ganoderma* mushroom. These events caused changes in some biomarkers associated with antioxidant responses.[72-73]

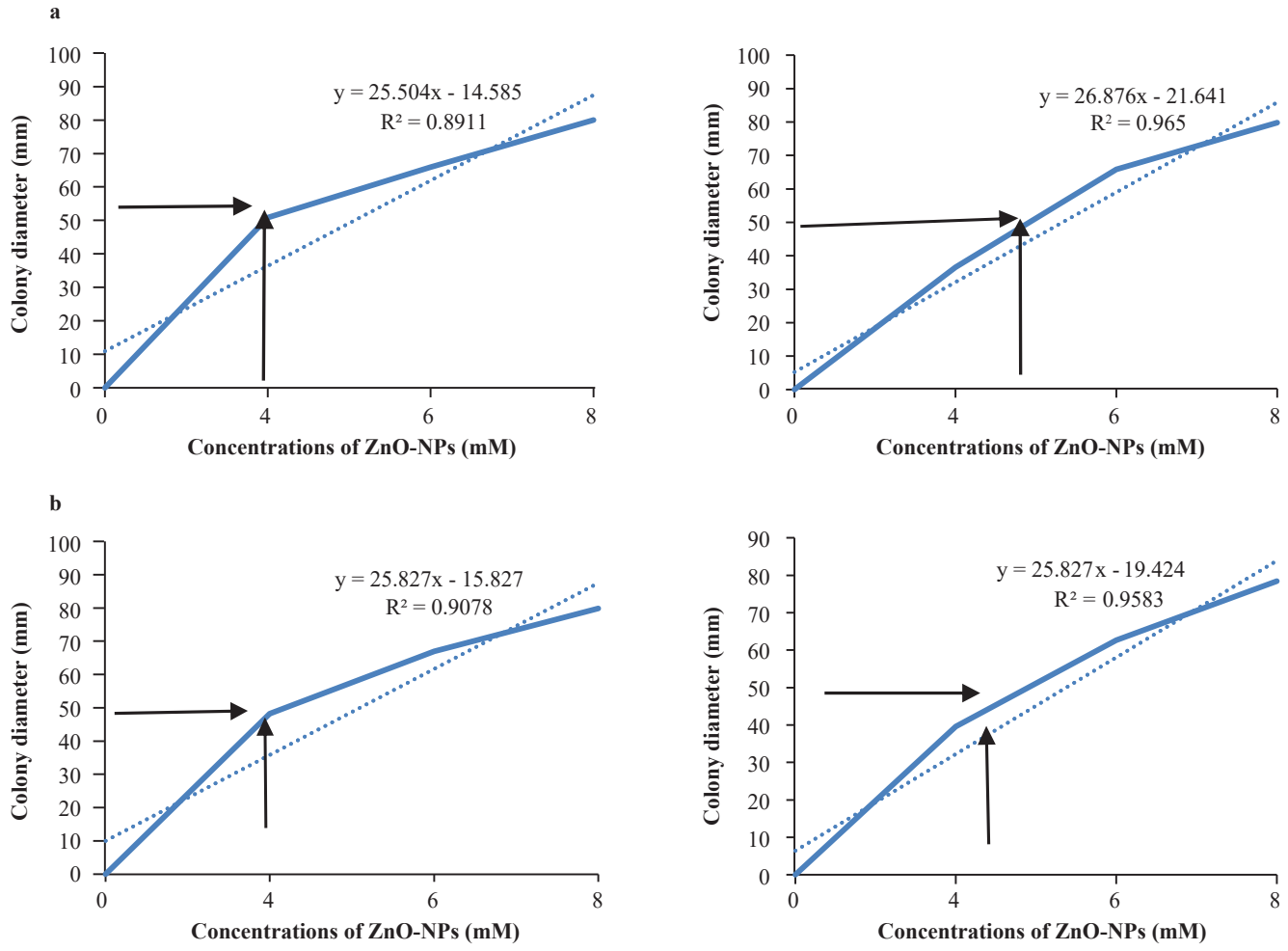

Figure 10. IC50 regression equations of different concentrations of ZnO and ZnONP on mycelial growth of G01 (a) and G16 (b) *Ganoderma lucidum* strains.

H_2O_2 content

This increase in H_2O_2 content can also be attributed to oxidative stress, resulting from exposure to heavy metals and a disturbance of metabolic balance by the resultant free radicals.[74] H_2O_2 is a major ROS that often plays a role in molecular signaling under different types of stress.[48] However, as the ROS increases to a level above the antioxidant capacity, it can cause serious damage to membrane functionality, which is associated with the inactivation of enzymes and disruption of the metabolic pathway, as well as mutations in DNA. These events affect physiological processes and can eventually cause cell death.[48]

In this research, increasing the ZnONPs concentration caused the H_2O_2 content to increase (Figure 7), which was consistent with previous research on the effects of bulk ZnO and ZnONPs on the H_2O_2 level and on biomarkers associated with antioxidant responses.[73]

Electrical conductivity (EC)

Stress from exposure to heavy metals can affect the permeability and structure of biological membranes. In turn, this can enhance the EC and cause interference with the absorption of nutrients. In the present research, ZnONPs and bulk ZnO increased the level of EC (Figure 7), due to the increase in ion leakage, whereby some biomarkers underwent changes that ultimately affected antioxidant reactions.[75] These are consistent with our results on *Ganoderma* mycelia. Membrane stability usually leads to an increase in membrane resistance, whereby stress is tolerated and homeostasis is maintained, thereby limiting the entry of nanoparticles into the cells.[50]

Activity of antioxidant enzymes

These enzymes could be involved in ROS scavenging to enable a better protection or homeostasis regulation in response to the stress caused by heavy metals.[52]

Rizwan et al. (2017)[65] reported that a low concentration of nanoparticles, including Al_2O_3-NPs, CeO_2-NPs and CuO-NP, stimulated the activity of antioxidant enzymes, but that their high concentrations reduced enzyme activity. The previous studies Shim et al. (2019)[74] and Garcia-Gomez et al. (2017)[33] reported similar observations and suggested that a higher concentration of AgNPs and ZnONPs could suppress the antioxidant system. In another study, Puthur (2016),[62] reported that high concentrations of bulk ZnO significantly reduced the CAT activity which may be due to the effect of free radicals on the protein section of the enzyme. It is suggested that the negative and toxic effects of nanoparticles are greater than those of their bulk counterparts, Shim et al. (2019),[74] which confirms our results (Figure 8 a, b, c), since it was observed that ZnONPs had a greater effect on *G. lucidum* mycelia than the effect of bulk ZnO at a high concentration. This may be attributed to the high adsorption or solubility of ionic species.[76] The high reactivity and solubility, along with the very small size of nanoparticles, increased their contact surface more than that of their bulk counterparts. Therefore, these particles showed a higher potential for inducing ROS production.[24]

Our findings revealed that supplementing the media of *G. lucidum* with ZnONPs and bulk ZnO could activate SOD, CAT and POD. Specifically, SOD was an enzyme involved in the antioxidant defense system, which dismutated the O_2^- anion into H_2O_2 and O_2. Since H_2O_2 remains toxic and should be removed from the cell,[50] the increase in CAT and POD are normally induced in the presence of H_2O_2,[77] so that it is decomposed into H_2O and O_2. In removing the H_2O_2 from respiratory pathways, the CAT enzyme plays a crucial role.[50] Thus, SOD, CAT and POD can prevent ROS toxicity by scavenging free radicals and by keeping them at low levels (Figure 8 and Figure 9).

CONCLUSION

ZnONPs were synthesized in a cost-effective and environmentally friendly manner by the seed extract of *Foeniculum vulgare*. The properties of nanoparticles were measured by UV–Vis spectroscopy, XRD, SEM, TEM, FT-IR and DLS. The results showed that ZnONPs and bulk ZnO increased ROS levels and had negative effects on growth factors of *G. lucidum* strains. A decline in growth-related indicators can be considered as a sign of toxicity caused by ZnONPs and bulk ZnO on *Ganoderma lucidum*. Both treatments increased the proline, MDA, EC and H_2O_2 contents. The activities of SOD, CAT, POD and antioxidant enzymes increased in response to low concentrations, but their levels decreased when higher concentrations of ZnONPs and bulk ZnO were used. Our research determined the appropriate concentrations of zinc types that had positive effects on the content of enzymatic antioxidants in *Ganoderma*. In general, the results showed that the application of ZnONPs and bulk ZnO reduced the growth of *Ganoderma* mycelia by creating oxidative stress but, ultimately, the mycelia reduced the oxidative stress by increasing the production of antioxidants. Among the treatments, ZnONPs had a greater effect on mycelia growth and on its antioxidant properties, compared to the effect of bulk ZnO. These treatments had a greater effect on the G16 strain than on the G01 strain.

ACKNOWLEDGMENTS

The authors would like to thank the University of Mohaghegh Ardabili Iran for providing financial support to this work.

CONFLICT OF INTEREST

The authors declare that they have no conflict of interest

FINANCIAL DISCLOSURE

The authors declared no financial interest.

ORCID IDS

M. Behnamian: https://orcid.org/0000-0001-8246-990X
A. Estaji: https://orcid.org/0000-0001-8365-4138

REFERENCES

1. Abd-Alwahab WI, Al-Dulaimi FK. Effects of kefir as a probiotic on total lipid profile and activity of aspartate amino transferase and alanine amino transferase in serum of human. Biochem Cell Arch. 2018;18:411–414. https://doi.org/10.13140/RG.2.2.16238.25928.
2. Ali SI, El-Emary GA, Mohamed AA. Effects of gamma irradiation on FT-IR fingerprint, phenolic contents and antioxidant activity of *Foeniculum vulgare* and *Carum carvi* seeds. Res J Pharm Technol. 2018;11(8):3323–3329. https://doi.org/10.5958/0974-360X.2018.00611.X.
3. Al-Jumaili MMO, Al-Dulaimi FK, Ajeel MA. The Role of *Ganoderma lucidum* Uptake on Some Hematological and Immunological Response in Patients with Coronavirus (COVID-19). Syst Rev Pharm. 2020;11(8):537–541.
4. Mohammadi Alagoz S, Ramezanzadeh Arvanaghi H, Dolatabadi N, Abbasi Khalaki M, Moameri M, Asgari Lajayer B, van Hullebusch ED. Chapter 15 - Impact on nutritional status of plants treated with nanoparticles. In: Rajput VD, Minkina T, Sushkova S, Mandzhieva SS, Rensing C (editors), *Toxicity of Nanoparticles in Plants*, vol. 5. Cambridge: Academic Press. 2022; pp 333–358. https://doi.org/10.1016/B978-0-323-90774-3.00005-2.
5. Fattahi N, Tabrizi BH, Rani S, Sadeghi Z, Dehghanian Z, Lajayer BA, van Hullebusch ED. Toxicity of nanoparticles onto plants: Overview of the biochemical and molecular mechanisms, Toxicity of nanoparticles in plants. Academic Press; 2022. p. 69–94. https://doi.org/10.1016/B978-0-323-90774-3.00002-7.
6. Arciniegas-Grijalba PA, Patiño-Portela MC, Mosquera-Sánchez LP, Guerrero-Vargas JA, Rodríguez-Páez JE. ZnO nanoparticles (ZnO-NPs) and their antifungal activity against coffee fungus *Erythricium salmonicolor*. Appl Nanosci. 2017;7(5):225–241. https://doi.org/10.1007/s13204-017-0561-3.
7. Arciniegas-Grijalba PA, Patiño-Portela MC, Mosquera-Sánchez LP, Guerra Sierra BE, Muñoz-Florez JE, Erazo-Castillo LA, Rodríguez-Páez JE. ZnO-based nanofungicides: Synthesis, characterization and their effect on the

coffee fungi *Mycena citricolor* and Colletotrichum sp. Mater Sci Eng C. 2019;98:808–825. https://doi.org/10.1016/j.msec.2019.01.031.

8. Mohammadi Arvanag F, Bayrami A, Habibi-Yangjeh A, Rahim Pouran S. A comprehensive study on antidiabetic and antibacterial activities of ZnO nanoparticles biosynthesized using *Silybum marianum* L seed extract. Mater Sci Eng C. 2019;97:397–405. https://doi.org/10.1016/j.msec.2018.12.058.
9. Aygün A, Özdemir S, Gülcan M, Cellat K, Şen F. Synthesis and characterization of Reishi mushroom-mediated green synthesis of silver nanoparticles for the biochemical applications J Pharm Biomed. 2020;178:112970. https://doi.org/10.1016/j.jpba.2019.112970.
10. Babaei K, Seyed Sharifi R, Pirzad A, Khalilzadeh R. Effects of bio fertilizer and nano Zn-Fe oxide on physiological traits, antioxidant enzymes activity and yield of wheat (*Triticum aestivum* L.) under salinity stress. J Plant Interact. 2017;12(1):381–389. https://doi.org/10.1080/17429145.2017.1371798.
11. Babich H, Stotzky G. Sensitivity of various bacteria including Actinomycetes and fungi to cadmium and the influence of pH on sensitivity. Appl Environ Microbiol. 1977;33(3):681–695. https://doi.org/10.1128/aem.33.3.681-695.1977.
12. Baldrian P. Interactions of heavy metals with white-rot fungi. Enzyme Microb Technol. 2003;32(1):78–91. https://doi.org/10.1016/S0141-0229(02)00245-4.
13. Bates LS, Waldren RP, Teare ID. Rapid determination of free proline for water-stress studies. Plant Soil. 1973;39(1):205–207. https://doi.org/10.1007/BF00018060.
14. Brown D, Donaldson K, Borm P, Schins R, Dehnhardt M, Gilmour P, Jimenez LA, Stone V. Calcium and ROS-mediated activation of transcription factors and TNF-alpha cytokine gene expression in macrophages exposed to ultrafine particles. Am J Physiol Lung Cell Mol Physiol. 2004;286(2):L344–L353. https://doi.org/10.1152/ajplung.00139.2003.
15. Cavello IA, Crespo JM, García SS, Zapiola JM, Luna MF, Cavalitto SF. Plant growth promotion activity of keratinolytic fungi growing on a recalcitrant waste known as "Hair Waste". Biotechnol Res Int. 2015;2015:952921. https://doi.org/10.1155/2015/952921.
16. Chandrasekaran R, Gnanasekar S, Seetharaman P, Keppanan R, Arockiaswamy W, Sivaperumal S. Formulation of Carica papaya latex-functionalized silver nanoparticles for its improved antibacterial and anticancer applications. J Mol Liq. 2016;219(c):232–238. https://doi.org/10.1016/j.molliq.2016.03.038.
17. Chapman SJ. The Uptake of Zinc by Selected Mushroom Fungi. Thesis. The Chinese University of Hong Kong, Shatin. New Territories Hong Kong, 1994
18. Chen W, Mai LQ, Peng JF, Xu Q, Zhu QY. FTIR study of vanadium oxide nanotubes from lamellar structure. J Mater Sci. 2004;39(7):2625–2627. https://doi.org/10.1023/B:JMSC.0000020044.67931.ad.
19. Choudhary MK, Kataria J, Sharma S. A biomimetic synthesis of stable gold nanoparticles derived from aqueous extract of *Foeniculum vulgare* seeds and evaluation of their catalytic activity. Appl Nanosci. 2017;7(7):439–447. https://doi.org/10.1007/s13204-017-0589-4.
20. Cör D, Knez Ž, Knez Hrnčič M. Antitumour, antimicrobial, antioxidant and antiacetylcholinesterase effect of *Ganoderma lucidum* terpenoids and polysaccharides: a review. Molecules. 2018;23(3):649. https://doi.org/10.3390/molecules23030649.
21. Darzian Rostami A, Yazdian F, Mirjani R, Soleimani M. Effects of different graphene-based nanomaterials as elicitors on growth and ganoderic acid production by *Ganoderma lucidum*. Biotechnol Prog. 2020;36(5):e3027. https://doi.org/10.1002/btpr.3027.
22. DeLay M. Microcantilever investigation of nanoconfinement effects on water transport. Biophys J. 1973;112(3):157a. https://doi.org/10.1016/j.bpj.2016.11.863.
23. Denny HJ, Wilkins DA. Zinc tolerance in *Betnlci* spp.IV. The mechanism of ectomycorrhizal amelioration of zinc toxicity. New Phytol. 1987;106: 533–545.
24. Devika V, Mohandass S, Nusrath T. Fourier transform infrared spectral studies of *foeniculum vulgare*. Int Res J Pharm. 2013;4(3):203–206. https://doi.org/10.7897/2230-8407.04343.
25. Dhindsa RS, Plumb-Dhindsa PAMELA, Thorpe TA. Leaf senescence: correlated with increased levels of membrane permeability and lipid peroxidation, and decreased levels of superoxide dismutase and catalase. J Exp Bot. 1981;32(1):93–101. https://doi.org/10.1093/jxb/32.1.93.
26. Dimitrijevic MV, Mitic VD, Cvetkovic JS, Stankov Jovanovic VP, Mutic JJ, Nikolic Mandic SD. Update on element content profiles in eleven wild edible mushrooms from family Boletaceae. Eur Food Res Technol. 2016;242(1):1–10. https://doi.org/10.1007/s00217-015-2512-0.
27. Du W, Sun Y, Ji R, Zhu J, Wu J, Guo H. TiO_2 and ZnO nanoparticles negatively affect wheat growth and soil enzyme activities in agricultural soil. J Environ Monit. 2011;13(4):822–828. https://doi.org/10.1039/c0em00611d.
28. Dutta S, Mitra M, Agarwal P, Mahapatra K, De S, Sett U, Roy S. Oxidative and genotoxic damages in plants in response to heavy metal stress and maintenance of genome stability. Plant Signal Behav. 2018;13(8):e1460048. https://doi.org/10.1080/15592324.2018.1460048.
29. Faizan M, Faraz A, Yusuf M, Khan ST, Hayat S. Zinc oxide nanoparticle-mediated changes in photosynthetic efficiency and antioxidant system of tomato plants. Photosynthetica. 2018;56(2):678–686. https://doi.org/10.1007/s11099-017-0717-0.
30. Gadd GM. Fungi and yeast for metal accumulation: microbial mineral recovery. New York: McGraw-Hill; 1990, pp 249–275.
31. Gao Y, Arokia Vijaya Anand M, Ramachandran V, Karthikkumar V, Shalini V, Vijayalakshmi S, Ernest D. Biofabrication of zinc oxide nanoparticles from *Aspergillus niger*, their antioxidant, antimicrobial and anticancer activity. J Cluster Sci. 2019;30(4):937–946. https://doi.org/10.1007/s10876-019-01551-6.
32. García-Gómez C, García S, Obrador AF, González D, Babín M, Fernández MD. Effects of aged ZnO NPs and soil type on Zn availability, accumulation and toxicity to pea and beet in a greenhouse experiment. Ecotoxicol Environ Saf. 2018;160:222–230. https://doi.org/10.1016/j.ecoenv.2018.05.019.
33. García-Gómez C, Obrador A, González D, Babín M, Fernández MD. Comparative effect of ZnO NPs, ZnO bulk and ZnSO4 in the antioxidant defences of two plant species growing in two agricultural soils under greenhouse conditions. Sci Total Environ. 2017;589:11–24. https://doi.org/10.1016/j.scitotenv.2017.02.153.
34. Gechev TS, Gadjev I, Van Breusegem F, Inzé D, Dukiandjiev S, Toneva V, Minkov I. Hydrogen peroxide protects tobacco from oxidative stress by inducing a set of antioxidant enzymes. Cell Mol Life Sci. 2002;59(4):708–714. https://doi.org/10.1007/s00018-002-8459-x.
35. Hassan SS, Abdel-Shafy HI, Mansour MS. Removal of pharmaceutical compounds from urine via chemical coagulation by green synthesized ZnO-nanoparticles followed by microfiltration for safe *reuse*. Arab J Chem. 2019;12(8):4074–4083. https://doi.org/10.1016/j.arabjc.2016.04.009.
36. Jan T, Iqbal J, Ismail M, Badshah N, Mansoor Q, Arshad A, Ahkam QM. Synthesis, physical properties and antibacterial activity of metal oxides nanostructures. Mater Sci Semicond Process. 2014;21:154–160. https://doi.org/10.1016/j.mssp.2014.01.006.
37. Khan ZU, Aisikaer G, Khan RU, Bu J, Jiang Z, Ni Z, Ying T. Effects of composite chemical pretreatment on maintaining quality in button mushrooms (*Agaricus bisporus*) during postharvest storage. Postharvest Biol Technol. 2014;95:36–41. https://doi.org/10.1016/j.postharvbio.2014.04.001.
38. Kokila K, Elavarasan N, Sujatha V. *Diospyros montana* leaf extract-mediated synthesis of selenium nanoparticles and their biological applications. New J Chem. 2017;41(15):7481–7490. https://doi.org/10.1039/C7NJ01124E.
39. Khan SA, Noreen F, Kanwal S, Iqbal A, Hussain G. Green synthesis of ZnO and Cu-doped ZnO nanoparticles from leaf extracts of *Abutilon indicum, Clerodendrum infortunatum, Clerodendrum inerme* and investigation of their biological and photocatalytic activities. Mater Sci Eng C. 2018;82:46–59. https://doi.org/10.1016/j.msec.2017.08.071.
40. Li C, Shi L, Chen D, Ren A, Gao T, Zhao M. Functional analysis of the role of glutathione peroxidase (GPx) in the ROS signaling pathway, hyphal branching and the regulation of ganoderic acid biosynthesis in *Ganoderma lucidum*. Fungal Genet Biol. 2015;82:168–180. https://doi.org/10.1016/j.fgb.2015.07.008.
41. Lingegowda DC, Kumar JK, Prasad AD, Zarei M, Gopal S. FTIR spectroscopic studies on Cleome gynandra–comparative analysis of functional group before and after extraction. Rom J Biophys. 2012;22(3-4):137–143.
42. Liu J, Liu S, Zhang X, Kan J, Jin C. Effect of gallic acid grafted chitosan film packaging on the postharvest quality of white button mushroom (*Agaricus bisporus*). Postharvest Biol Technol. 2019;147:39–47. https://doi.org/10.1016/j.postharvbio.2018.09.004.
43. Wang Y, Mo Y, Li D, Xiang C, Jiang Z, Wang J. The main factors inducing postharvest lignification in king oyster mushrooms (*Pleurotus eryngii*): wounding and ROS-mediated senescence. Food Chem. 2019;301:125224. https://doi.org/10.1016/j.foodchem.2019.125224.

44. Liu Q, Kong W, Hu S, Kang Y, Zhang Y, Ng TB. Effects of *Oudemansiella radicata* polysaccharide on postharvest quality of oyster mushroom (*Pleurotus ostreatus*) and its antifungal activity against *Penicillium digitatum*. Postharvest Biol Technol. 2020;166:111207. https://doi.org/10.1016/j.postharvbio.2020.111207.
45. Long TC, Saleh N, Tilton RD, Lowry GV, Veronesi B. Titanium dioxide (P25) produces reactive oxygen species in immortalized brain microglia (BV2): implications for nanoparticle neurotoxicity. Environ Sci Technol. 2006;40(14):4346–4352. https://doi.org/10.1021/es060589n.
46. Xia T, Kovochich M, Liong M, Madler L, Gilbert B, Shi H, Yeh JI, Zink JI, Nel AE. Comparison of the mechanism of toxicity of zinc oxide and cerium oxide nanoparticles based on dissolution and oxidative stress properties. ACS Nano. 2008;2(10):2121–2134. https://doi.org/10.1021/nn800511k.
47. Zhou W, Leul M, Leul M. Uniconazole-induced alleviation of freezing injury in relation to changes in hormonal balance, enzyme activities and lipid peroxidation in winter rape. Plant Growth Regul. 1998;26(1):41–47. https://doi.org/10.1023/A:1006004921265.
48. Singh A, Singh NB, Hussain I, Singh H, Yadav V, Singh SC. Green synthesis of nano zinc oxide and evaluation of its impact on germination and metabolic activity of *Solanum lycopersicum*. J Biotechnol. 2016;233:84–94. https://doi.org/10.1016/j.jbiotec.2016.07.010.
49. Hafeez M, Shaheen R, Akram B, Ahmed MN, ul-Abdin Z, Haq S, Din SU, Zeb M, Khan MA. Green Synthesis of Nickel Oxide Nanoparticles using Populus ciliata Leaves Extract and their Potential Antibacterial Applications. S Afr J Chem. 2021;75:168–173. https://doi.org/10.17159/0379-4350/2021/v75a21.
50. Singh J, Kumar S, Alok A, Upadhyay SK, Rawat M, Tsang DC, Bolan N, Kim KH. The potential of green synthesized zinc oxide nanoparticles as nutrient source for plant growth. J Clean Prod. 2019;214:1061–1070. https://doi.org/10.1016/j.jclepro.2019.01.018.
51. Nascimento CP, Luz DA, da Silva CCS, Malcher CMR, Fernandes LMP, Dalla Santa HS, Gomes ARQ, Monteiro MC, Ribeiro CHMA, Fontes-Júnior EA, et al. *Ganoderma lucidum* Ameliorates Neurobehavioral Changes and Oxidative Stress Induced by Ethanol Binge Drinking. Oxid Med Cell Longev. 2020;2020(11):1–12. https://doi.org/10.1155/2020/2497845.
52. Matute RG, Serra A, Figlas D, Curvetto N. Copper and zinc bioaccumulation and bioavailability of *Ganoderma lucidum*. J Med Food. 2011;14(10):1273–1279. https://doi.org/10.1089/jmf.2010.0206.
53. Merchant SS. The elements of plant micronutrients. Plant Physiol. 2010;154(2):512–515. https://doi.org/10.1104/pp.110.161810.
54. Moncalvo JM. Systematics of Ganoderma. In: Flood J (editor), *Ganoderma Diseases of Perennial Crops*. CABI Publishing; 2000. pp 23–45. https://doi.org/10.1079/9780851993881.0023.
55. Rao S, Shekhawat GS. Toxicity of ZnO engineered nanoparticles and evaluation of their effect on growth, metabolism and tissue specific accumulation in *Brassica juncea*. J Environ Chem Eng. 2014;2(1):105–114. https://doi.org/10.1016/j.jece.2013.11.029.
56. Ogunyemi SO, Abdallah Y, Zhang M, Fouad H, Hong X, Ibrahim E, Masum MMI, Hossain A, Mo J, Li B. Green synthesis of zinc oxide nanoparticles using different plant extracts and their antibacterial activity against Xanthomonas oryzae pv. oryzae. Artif Cells Nanomed Biotechnol. 2019;47(1):341–352. https://doi.org/10.1080/21691401.2018.1557671.
57. Oniszczuk T, Combrzyński M, Matwijczuk A, Oniszczuk A, Gładyszewska B, Podleśny J, Czernel G, Karcz D, Niemczynowicz A, Wójtowicz A. Physical assessment, spectroscopic and chemometric analysis of starch-based foils with selected functional additives. PLoS One. 2019;14(2):e0212070. https://doi.org/10.1371/journal.pone.0212070.
58. Petrov V, Hille J, Mueller-Roeber B, Gechev TS. ROS-mediated abiotic stress-induced programmed cell death in plants. Front Plant Sci. 2015;6(69):69. https://doi.org/10.3389/fpls.2015.00069.
59. Płaza G, Łukasik W, Ulfig K. Effect of cadmium on growth of potentially pathogenic soil fungi. Mycopathologia. 1998;141(2):93–100. https://doi.org/10.1023/A:1006991306756.
60. Mateo D, Morales P, Ávalos A, Haza AI. Comparative cytotoxicity evaluation of different size gold nanoparticles in human dermal fibroblasts. J Exp Nanosci. 2015;10(18):1401–1417. https://doi.org/10.1080/17458080.2015.1014934.
61. Poynton HC, Lazorchak JM, Impellitteri CA, Smith ME, Rogers K, Patra M, Hammer KA, Allen HJ, Vulpe CD. Differential gene expression in Daphnia magna suggests distinct modes of action and bioavailability for ZnO nanoparticles and Zn ions. Environ Sci Technol. 2011;45(2):762–768. https://doi.org/10.1021/es102501z.
62. Puthur JT. Antioxidants and cellular antioxidation mechanism in plants. South Indian J Biol Sci. 2016;2(1):9–13. https://doi.org/10.22205/sijbs/2016/v2/i1/100335.
63. Ray PD, Huang BW, Tsuji Y. Reactive oxygen species (ROS) homeostasis and redox regulation in cellular signaling. Cell Signal. 2012;24(5):981–990. https://doi.org/10.1016/j.cellsig.2012.01.008.
64. Ben Rejeb K, Abdelly C, Savouré A. How reactive oxygen species and proline face stress together. Plant Physiol Biochem. 2014;80:278–284. https://doi.org/10.1016/j.plaphy.2014.04.007.
65. Rizwan M, Ali S, Qayyum MF, Ok YS, Adrees M, Ibrahim M, Zia-ur-Rehman M, Farid M, Abbas F. Effect of metal and metal oxide nanoparticles on growth and physiology of globally important food crops: A critical review. J Hazard Mater. 2017;322:2–16. https://doi.org/10.1016/j.jhazmat.2016.05.061.
66. Rothstein A, Hayes AD. The relationship of the cell surface to metabolism. XIII. The cation-binding properties of the yeast cell surface. Arch Biochem Biophys. 1956;63(1):87–99. https://doi.org/10.1016/0003-9861(56)90012-1.
67. Sajadi SM, Nasrollahzadeh M, Maham M. Aqueous extract from seeds of *Silybum marianum* L. as a green material for preparation of the Cu/Fe3O4 nanoparticles: a magnetically recoverable and reusable catalyst for the reduction of nitroarenes. J Colloid Interface Sci. 2016;469:93–98. https://doi.org/10.1016/j.jcis.2016.02.009.
68. Sánchez C. Reactive oxygen species and antioxidant properties from mushrooms. Synth Syst Biotechnol. 2017;2(1):13–22. https://doi.org/10.1016/j.synbio.2016.12.001.
69. Matinise N, Fuku XG, Kaviyarasu K, Mayedwa N, Maaza M. ZnO nanoparticles via Moringa oleifera green synthesis: physical properties and mechanism of formation. Appl Surf Sci. 2017;406:339–347. https://doi.org/10.1016/j.apsusc.2017.01.219.
70. Sari MG, Saeb MR, Shabanian M, Khaleghi M, Vahabi H, Vagner C, Zarrintaj P, Khalili R, Paran SMR, Ramezanzadeh B, et al. Epoxy/starch-modified nano-zinc oxide transparent nanocomposite coatings: A showcase of superior curing behavior. Prog Org Coat. 2018;115:143–150. https://doi.org/10.1016/j.porgcoat.2017.11.016.
71. Selim YA, Azb MA, Ragab I, Abd El-Azim MHM. Green synthesis of zinc oxide nanoparticles using aqueous extract of *Deverra tortuosa* and their cytotoxic activities. Sci Rep. 2020;10(3445):1–9. https://doi.org/10.1038/s41598-020-60541-1.
72. Sewelam N, Kazan K, Schenk PM. Global plant stress signaling: reactive oxygen species at the cross-road. Front Plant Sci. 2016;7(187):1–21. https://doi.org/10.3389/fpls.2016.00187.
73. Sharmila G, Thirumarimurugan M, Muthukumaran C. Green synthesis of ZnO nanoparticles using *Tecoma castanifolia* leaf extract: characterization and evaluation of its antioxidant, bactericidal and anticancer activities. Microchem J. 2019;145:578–587. https://doi.org/10.1016/j.microc.2018.11.022.
74. Shim YJ, Soshnikova V, Anandapadmanaban G, Mathiyalagan R, Jimenez Perez ZE, Markus J, Ju Kim Y, Castro-Aceituno V, Yang DC. Zinc oxide nanoparticles synthesized by *Suaeda japonica* Makino and their photocatalytic degradation of methylene blue. Optik (Stuttg). 2019;182:1015–1020. https://doi.org/10.1016/j.ijleo.2018.11.144.
75. Singh J, Dutta T, Kim KH, Rawat M, Samddar P, Kumar P. 'Green'synthesis of metals and their oxide nanoparticles: applications for environmental remediation. J Nanobiotechnology. 2018;16(1):84. https://doi.org/10.1186/s12951-018-0408-4.
76. Siripireddy B, Mandal BK. Facile green synthesis of zinc oxide nanoparticles by Eucalyptus globulus and their photocatalytic and antioxidant activity. Adv Powder Technol. 2017;28(3):785–797. https://doi.org/10.1016/j.apt.2016.11.026.
77. Smirnoff N, Arnaud D. Hydrogen peroxide metabolism and functions in plants. New Phytol. 2019;221(3):1197–1214. https://doi.org/10.1111/nph.15488.